Manuscript Title

This manuscript ([permalink](#)) was automatically generated from [greenelab/mpmp-manuscript@f567ead](#) on May 27, 2021.

Authors

- **John Doe**
  ⓘD [XXXX-XXXX-XXXX-XXXX](#) · [johndoe](#) · [johndoe](#)
  Department of Something, University of Whatever · Funded by Grant XXXXXXXX

- **Jane Roe**
  ⓘD [XXXX-XXXX-XXXX-XXXX](#) · [janeroe](#)
  Department of Something, University of Whatever; Department of Whatever, University of Something

Abstract

Introduction

Although cancer can be initiated and driven by many different genetic alterations, these tend to converge on a limited number of pathways or signaling processes [1]. A comprehensive understanding of how diverse genetic alterations perturb these central pathways is vital to precision medicine and biomarker identification efforts, as driver mutation status alone confers limited prognostic information [2,3]. While many methods exist to distinguish driver mutations from passenger mutations based on genomic sequence characteristics [4,5,6], until recently it has been a challenge to connect driver mutations to downstream changes in gene expression and cellular function within individual tumor samples.

The Cancer Genome Atlas (TCGA) Pan-Cancer Atlas provides uniformly processed, multi-platform -omics measurements across tens of thousands of samples from 33 cancer types [7]. Enabled by this publicly available data, a growing body of work on linking the presence of driving genetic alterations in cancer to downstream gene expression changes has emerged. Recent studies have considered Ras pathway alteration status in colorectal cancer [8], alteration status across many cancer types in Ras genes [9,10], TP53 [11], and PIK3CA [12], and alteration status across cancer types in frequently mutated genes [13]. More broadly, other groups have drawn on similar ideas to distinguish between the functional effects of different alterations in the same driver gene [14], to link alterations with similar gene expression signatures within cancer types [15], and to identify trans-acting expression quantitative trait loci (trans-eQTLs) in germline genetic studies [16].

These studies share a common thread: they each combine genomic (point mutation and copy number variation) data with transcriptomic (RNA sequencing) data within samples to interrogate the functional effects of genetic variation. RNA sequencing is ubiquitous and cheap, and its experimental and computational methods are relatively mature, making it a vital tool for generating insight into cancer pathology [17]. Some driver mutations, however, are known to act indirectly on gene expression through varying mechanisms. For example, oncogenic IDH1 and IDH2 mutations in glioma have been shown to interfere with histone demethylation, which results in increased DNA methylation and blocked cell differentiation [18,19]. Other genes implicated in aberrant DNA methylation in cancer include the TET family of genes [20] and SETD2 [21]. Certain driver mutations, such as those in DNA damage repair genes, may lead to detectable patterns of somatic mutation [22]. Additionally, correlation between gene expression and protein abundance in cancer cell lines is limited, and proteomics data could correspond more directly to certain cancer phenotypes and pathway perturbations [23]. In these contexts and others, integrating different data modalities or combining multiple data modalities could be more effective than relying solely on gene expression as a functional signature.

Here, we seek to compare -omics data types profiled in the TCGA Pan-Cancer Atlas for use as a multivariate functional readout of genetic alterations in cancer. We focus on DNA methylation (27K and 450K probe chips), reverse phase protein array (RPPA), and mutational signatures data [24] as alternative readouts. Prior studies have identified univariate correlations of CpG site methylation [25,26] and correlations of RPPA protein profiles [27] with the presence or absence of certain driver mutations. Other relevant past work includes linking point mutations and copy number variants (CNVs) with changes in methylation and expression at individual genes [28,29] and identifying functional modules that are perturbed by somatic mutations [30,31]. However, no direct comparison has been made between different data types for this application, particularly in the multivariate case where we consider changes to -omics-derived gene signatures rather than individual genes in isolation.

We select a collection of potential cancer drivers with varying functions and roles in cancer development [32]. We use mutation status in these genes as labels to train classifiers, using each of the data types listed as training data, in a pan-cancer setting; we follow similar methods to the elastic net logistic regression approach described in Way et al. 2018 [9] and Way et al. 2020 [13]. We show that there is considerable predictive signal for many genes relative to a random baseline, and that gene expression and DNA methylation generally provide the best predictions of mutation state. Surprisingly, we find that across a variety of target genes, they are approximately equally effective predictors; the target gene, rather than the data type, is the primary determinant of performance. In addition, we observe that combining data types into a single multi-omics model provides little, if any, performance benefit over the most performant model using a single data type. Our results will help to inform the design of future functional genomics studies in cancer, suggesting that for many strong drivers with clear functional signatures, gene expression and DNA methylation measurements provide similar information content.

Methods

Mutation data download and preprocessing

To generate binary mutated/non-mutated gene labels for our machine learning model, we used mutation calls for TCGA samples from MC3 [33] and copy number threshold calls from GISTIC2.0 [34]. MC3 mutation calls were downloaded from the Genome Data Commons (GDC) of the National Cancer Institute, at `https://gdc.cancer.gov/about-data/publications/pancanatlas` . Copy number threshold calls are from an older version of PanCanAtlas, and are available here: `https://figshare.com/articles/dataset/TCGA_PanCanAtlas_Copy_Number_Data/614412 2` . We removed hypermutated samples (defined as five or more standard deviations above the mean non-silent somatic mutation count) from our dataset to reduce the number of false positives (i.e., non-driver mutations). In total, this resulted in 9,074 TCGA samples with mutation and copy number data. Any sample with a non-silent somatic variant in the target gene was included in the positive set. We also included copy number gains in the target gene for oncogenes, and copy number losses in the target gene for tumor suppressor genes, in the positive set; all remaining samples were considered negative for mutation in the target gene.

Omics data download and preprocessing

RNA sequencing, 27K and 450K methylation array, and RPPA datasets for TCGA samples were all downloaded from GDC, at the same link provided above. Mutational signatures information for TCGA samples with whole-exome sequencing data was downloaded from the International Cancer Genome Consortium (ICGC) data portal, at `https://dcc.icgc.org/releases/PCAWG/mutational_signatures/Signatures_in_Sample s/SP_Signatures_in_Samples` . For our experiments, we used only the "single base signature" (SBS) mutational signatures, generated in [24]. We standardized (took z-scores of) each column of RNA sequencing and RPPA data; methylation data and mutational signatures data were left untransformed (beta values and mutation counts respectively), except in multi-omics experiments where all data types were standardized. For the RNA sequencing dataset, we used only the top 8,000 gene features by mean absolute deviation as predictors in our models, except in multi-omics experiments where all 15,639 genes were used.

In order to remove missing values from the methylation datasets, we removed the 10 samples with the most missing values, then performed mean imputation for probes with 1 or 2 values missing. All probes with missing values remaining after sample filtering and imputation were dropped from the analysis. This left us with 20,040 CpG probes in the 27K methylation dataset, and 370,961 CpG probes in the 450K methylation dataset. For experiments where "raw" methylation data was used, we used

the top 100,000 probes in the 450K dataset by mean absolute deviation for computational efficiency, and we used all of the 20,040 probes in the 27K dataset. For experiments where "compressed" methylation data was used, we used principal component analysis (PCA), as implemented in the `scikit-learn` Python library [35], to extract the top 5,000 principal components from the methylation datasets. We initially applied the beta-mixture quantile normalization (BMIQ) method [36] to correct for variability in signal intensity between type I and type II probes, but we observed that this had no effect on our results. We report uncorrected results in the main paper for simplicity.

Comparing data modalities

We made three main comparisons in this study, listed in the results section: one between different sets of genes using only expression data, one comparing expression and DNA methylation data types, and one comparing all data types. This was mainly due to sample size limitations – running a single comparison using all data types would force us to use only samples that are profiled for every data type, which would discard a large number of samples that lack profiling on only one or a few data types. Thus, for each of the three comparisons, we used the intersection of TCGA samples having measurements for all of the datasets being compared in that experiment. This resulted in three distinct sets of samples: 9,074 samples shared between {expression, mutation} data, 7,981 samples shared between {expression, mutation, 27K methylation, 450K methylation}, and 5,226 samples shared between {expression, mutation, 27K methylation, 450K methylation, RPPA, microRNA, mutational signatures}. When we dropped samples between experiments as progressively more data types were added, we observed that the dropped samples had approximately the same cancer type proportions as the dataset as a whole. In other words, samples that were profiled for one data type but not another did not tend to come exclusively from one or a few cancer types. Exceptions included acute myeloid leukemia (LAML) which had no samples profiled in the RPPA data, and ovarian cancer (OV) which had only 8 samples with 450K methylation data. More detailed information on cancer type proportions profiled for each data type is provided in (the supplement).

For each target gene, in order to ensure that the training dataset was reasonably balanced (i.e. that there would be enough mutated samples to train an effective classifier), we included only cancer types with at least 15 mutated samples and at least 5% mutated samples, which we refer to here as "valid" cancer types. After applying these filters, the number of valid cancer types remaining for each gene varied based on the set of samples used: more data types resulted in fewer shared samples, and fewer samples generally meant fewer valid cancer types. In some cases, this resulted in genes with no valid cancer types, which we dropped from the analysis. Out of the 127 genes from the original cancer gene set described in Vogelstein et al. 2013 [32], for the analysis using {expression, mutation} data we retained 85 target genes, for the {expression, mutation, 27k methylation, 450k methylation} analysis we retained 84 genes, and for the analysis using all data types we retained 75 genes.

We additionally explored mutation prediction from gene expression alone using 3 gene sets of equal size: the cancer-related genes from Vogelstein et al. 2013 described above, a set of frequently mutated genes in TCGA, and a set of random genes with mutations profiled by MC3. To match the size of the Vogelstein et al. gene set, we took the 85 most frequently mutated genes in TCGA as quantified by MC3, all of which had at least one valid cancer type. For the random gene set, we first filtered to the set of all genes with 2 or more valid cancer types by the above criteria, then sampled 85 of these genes uniformly at random. Based on the results of the gene expression experiments, we used the Vogelstein et al. gene set for all subsequent experiments comparing -omics data types.

Training classifiers to detect cancer mutations

We trained logistic regression classifiers to predict whether or not a given sample has a mutational event in a given target gene, using data from various -omics datasets as explanatory variables. Our

model is trained on -omics data (X) to predict mutation presence or absence (y) in a target gene. To control for varying mutation burden per sample, and to adjust for potential cancer type-specific expression patterns, we included one-hot encoded cancer type and $\log_{10}$(sample mutation count) in the model as covariates. Since our -omics datasets tend to have many dimensions and comparatively few samples, we used an elastic net penalty to prevent overfitting [37], in line with the approach used in Way et al. 2018 [9] and Way et al. 2020 [13]. Elastic net logistic regression finds the feature weights $\hat{w} \in \mathbb{R}^p$ solving the following optimization problem:

$$\hat{w} = \operatorname{argmin}_w \ell(X, y; w) + \alpha\lambda||w||_1 + \frac{1}{2}\alpha(1-\lambda)||w||_2$$

where $i \in \{1, \ldots, n\}$ denotes a sample in the dataset, $X_i \in \mathbb{R}^p$ denotes features (omics measurements) from the given sample, $y_i \in \{0, 1\}$ denotes the label (mutation presence/absence) for the given sample, and $\ell(\cdot)$ denotes the negative log-likelihood of the observed data given a particular choice of feature weights, i.e.

$$\ell(X, y; w) = -\sum_{i=1}^{n} y_i \log\left(\frac{1}{1 + e^{-w^\top X_i}}\right) + (1 - y_i) \log\left(1 - \frac{1}{1 + e^{-w^\top X_i}}\right)$$

This optimization problem leaves two hyperparameters to select: α (controlling the tradeoff between the data log-likelihood and the penalty on large feature weight values), and λ (controlling the tradeoff between the L1 penalty and L2 penalty on the weight values). Although the elastic net optimization problem does not have a closed form solution, the loss function is convex, and iterative optimization algorithms are commonly used for finding reasonable solutions. For fixed values of α and λ, we solved for $\hat{w}$ using stochastic gradient descent, as implemented in `scikit-learn`'s `SGDClassifier` method.

Given weight values $\hat{w}$, it is straightforward to predict the probability of a positive label (mutation in the target gene) $P(y^* = 1 \mid X^*; \hat{w})$ for a test sample X^*:

$$P(y^* = 1 \mid X^*; \hat{w}) = \frac{1}{1 + e^{-\hat{w}^\top X^*}}$$

and the probability of no mutation in the target gene, $P(y^* = 0 \mid X^*; \hat{w})$, is given by (1 - the above quantity).

For each target gene, we evaluated model performance using 2 replicates of 4-fold cross-validation, where train and test splits were stratified by cancer type and sample type. That is, each training set/test set combination had equal proportions of each cancer type (BRCA, SKCM, COAD, etc) and each sample type (primary tumor, recurrent tumor, etc). To choose the elastic net hyperparameters, we used 3-fold nested cross-validation, with a grid search over the following hyperparameter ranges: λ = [0.0, 0.05, 0.1, 0.3, 0.5, 0.7, 0.9, 1.0] and α = [0.0001, 0.001, 0.01, 0.1, 1, 10]. Using the grid search results, for each evaluation fold we selected the set of hyperparameters with the optimal area under the precision-recall curve (AUPR), averaged over the three inner folds.

Although we stratified our train and test datasets for cancer type and sample type, we opted not to stratify by label. In other words, we did not ensure that cross-validation splits had proportions of positive (mutated) and negative (non-mutated) samples that were exactly equal to each other; we instead sampled randomly with respect to labels. Label-stratified cross-validation chooses test sets that have exactly the same label balance as the training set, which could select a model that is less robust to shifts in the label proportion than one that is trained and evaluated without controlling label

balance. Particularly for the problem of mutation prediction, the proportion of samples that are mutated in a given cancer type or subtype often varies considerably, which makes robustness across variation in label proportions important.

Evaluating mutation prediction classifiers

To quantify classification performance for a continuous or probabilistic output, such as that provided by logistic regression, the area under the receiver-operator curve (AUROC) [38] and the area under the precision-recall curve (AUPR) [39] metrics are frequently used. These metrics summarize performance across a variety of binary label thresholds, rather than requiring choice of a single threshold to determine positive or negative predictions. In the main text, we report results using AUPR, summarized using average precision. AUPR has been shown to distinguish between models more accurately than AUROC when there are few positively labeled samples [40,41]. As an additional correction for imbalanced labels, in many of the results in the main text we report the difference in AUPR between a classifier fit to true mutation labels, and a classifier fit to data where the mutation labels are randomly shuffled. In cases where mutation labels are highly imbalanced (very few mutated samples and many non-mutated samples), a classifier with shuffled labels may perform well simply by chance, e.g. by predicting the negative/non-mutated class for most samples. To maintain the same label balance for the classifiers with shuffled labels as the classifiers with the true labels, we shuffled labels separately in the train and test sets for each cross-validation split.

Recall that for each target gene and each -omics dataset, we ran 2 replicates of 4-fold cross-validation, for a total of 8 performance results. To make a statistical comparison between two models using these performance distributions, we used paired-sample *t*-tests, where performance measurements derived from the same cross-validation fold are considered paired measurements. We used this approach to compare a model trained on true labels with a model trained on shuffled labels (addressing the question, "for the given gene using the given data type, can we predict mutation status better than random"), and to compare a model trained on data type A with a model trained on data type B (addressing the question, "for the given gene, can we make more effective mutation status predictions using data type A or data type B"). We corrected for multiple tests using a Benjamini-Hochberg false discovery rate correction. For all of our experiments, we set a conservative corrected threshold of $p = 0.001$; we were able to estimate the number of false positives by examining genes with better performance for shuffled mutation labels than true labels. We chose our threshold to ensure that none of these genes were considered significant, since we would never expect permuting labels to improve performance. However, our results were not sensitive to the choice of this threshold.

Multi-omics prediction experiments

To predict mutation presence or absence in cancer genes using multiple data types simultaneously, we concatenated individual datasets into a large feature matrix, then used the same elastic net logistic regression method described previously. For this task, we considered only the gene expression, 27K methylation, and 450K methylation datasets. We used only these data types to limit the number of multi-omics combinations: the expression and methylation datasets resulted in the best overall performance across the single-omics experiments so we limited combinations to those datasets here. For gene expression we used all 15,639 genes available in our RNA sequencing dataset, for the 27K methylation dataset we used all 20,040 CpG probes, and for the 450K methylation dataset we used the top 5,000 principal components.

To construct the multi-omics models, we considered each of the pairwise combinations of the datasets listed above, as well as a combination of all 3 datasets. When combining multiple datasets, we concatenated along the column axis, including covariates for cancer type and sample mutation

burden as before. For all multi-omics experiments, we used only the samples from TCGA with data for all three data types (i.e. the same 7,981 samples used in the single-omics experiments comparing expression and methylation data types). Due to computational demands, we considered only a limited subset of the Vogelstein et al. genes as target genes, including EGFR, IDH1, KRAS, PIK3CA, SETD2 and TP53. We selected these genes because we have previously observed that they have good predictive performance, and they represent a combination of alterations that have strong gene expression signatures (KRAS, EGFR, IDH1, TP53) and strong DNA methylation signatures (IDH1, SETD2, TP53 to some degree).

Data and code availability

All analyses were implemented in the Python programming language and are available in the following GitHub repository: `https://github.com/greenelab/mpmp` , under the open-source BSD 3-clause license. Scripts to download large data files from GDC and other sources are located in the `00_download_data` directory. Scripts to run experiments comparing data modalities used individually are located in the `02_classify_mutations` directory, and scripts to run multi-omics experiments are located in the `05_classify_mutations_multimodal` directory. The Python environment was managed using `conda` , and directions for setting up the environment can be found in the `README.md` file. All analyses were run locally on a CPU.

Results

Using diverse data modalities to predict cancer alterations

We collected five different data modalities from cancer samples in the TCGA Pan-Cancer Atlas, capturing five steps of cellular function that are perturbed by genetic alterations in cancer (Figure 1A). These included gene expression (RNA-seq data), DNA methylation (27K and 450K Illumina BeadChip arrays), protein abundance (RPPA data), microRNA expression data, and patterns of somatic mutation (mutational signatures). To link these diverse data modalities to changes in mutation status, we used elastic net logistic regression to predict the presence or absence of mutations in cancer genes, using these readouts as predictive features (Figure 1B). We evaluated the resulting mutation status classifiers in a pan-cancer setting, preserving the proportions of each of the 33 cancer types in TCGA for 8 train/test splits (4 folds x 2 replicates) in each of 85 cancer genes (Figure 1C).

We sought to compare classifiers against a baseline where mutation labels are permuted (to identify genes whose mutation status correlates strongly with a functional signature in a given data type), and also to compare classifiers trained on true labels across different data types (to identify data types that are more or less predictive of mutations in a given gene). To account for variation between dataset splits in making these comparisons, we treat classification metrics from the 8 train/test splits as performance distributions, which we compare using t-tests. We summarize performance across all genes in our cancer gene set using a similar approach to a volcano plot, in which each point is a gene. In our summary plots, the x-axis shows the magnitude of the change in the classification metric between conditions, and the y-axis shows the p-value for the associated t-test. Figure 1C illustrates this evaluation pipeline.
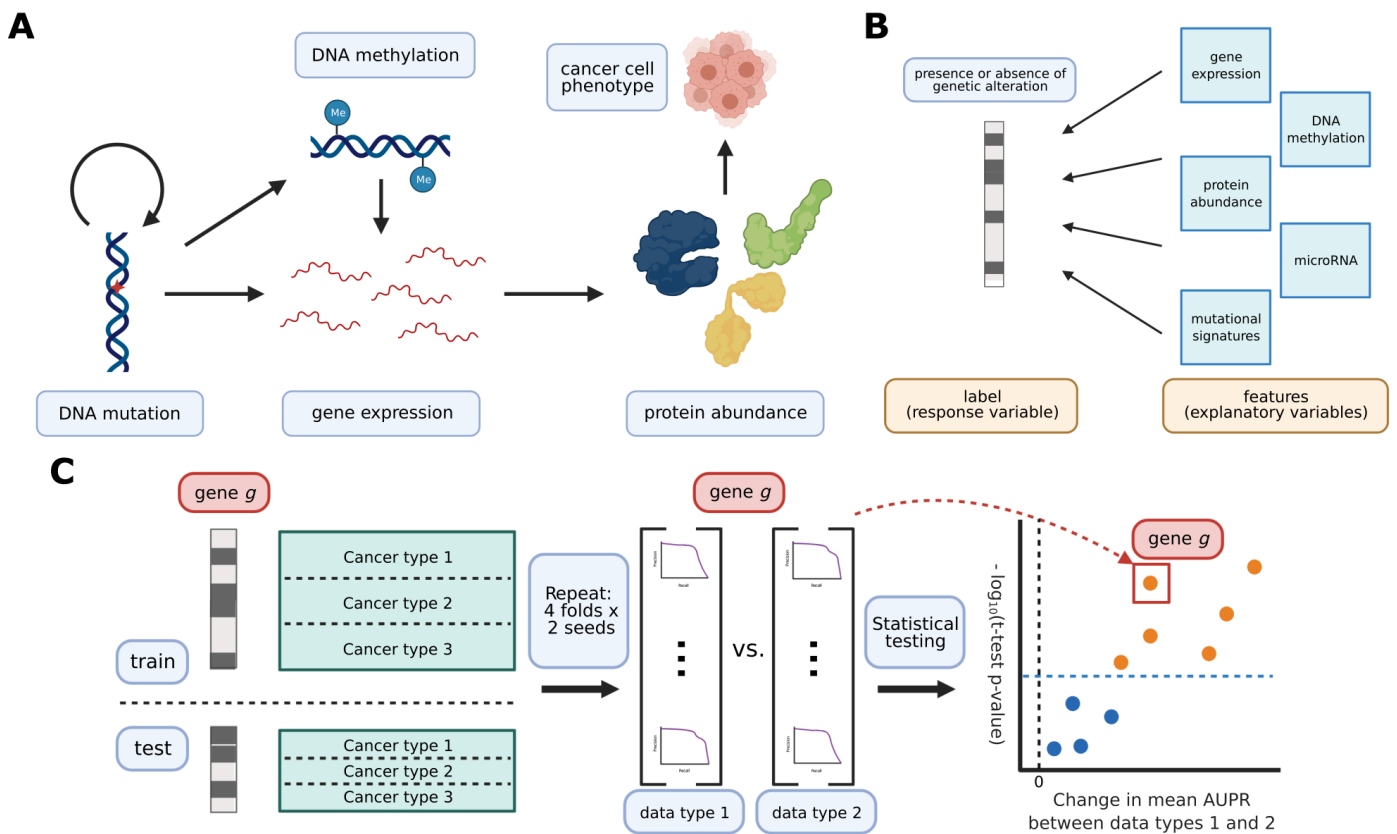
Figure 1: A. Cancer mutations can perturb cellular function via a variety of cellular processes. Arrows represent major potential paths of information flow from a somatic mutation in DNA to its resulting cell phenotype; circular arrow represents the ability of certain mutations (e.g. in DNA damage repair genes) to alter somatic mutation patterns. Note that this does not reflect all possible relationships between cellular processes: for instance, changes in gene expression can lead to changes in somatic mutation rates. **B.** Predicting presence/absence of somatic alterations in cancer from diverse data modalities. In this study, we use functional readouts from TCGA as predictive features and the presence or absence of mutation in a given gene as labels. This reverses the primary direction of information flow shown in Panel A. **C.** Schematic of evaluation pipeline.

Selection of cancer-related genes improves predictive signal

As a baseline, we evaluated prediction of mutation status from gene expression data across several different gene sets. Past work has evaluated mutation prediction for the top 50 most mutated genes in TCGA [13], and we sought to extend this to a broader list of gene sets. We compared a set of cancer-related genes from Vogelstein et al. 2013 [32] with a set of random genes having equal size, and a set of the most mutated genes in TCGA having equal size. For all gene sets, we used only the set of TCGA samples for which both gene expression and somatic mutation data exists, resulting in a total of 9,074 samples from all 33 cancer types (Figure 2A). This set of samples was further filtered for each target gene to cancer types containing at least 15 mutated samples and at least 5% of samples mutated for that cancer type. We then evaluated the performance for each target gene in each of the three gene sets.

Figure 2B summarizes performance for all genes in each gene set. Genes from the Vogelstein et al. set were more predictable than randomly chosen genes or those selected by total mutation count. Figures 2C, 2D, and 2E show performance for each gene in the random gene set, most mutated gene set, and Vogelstein et al. gene set respectively. In total, for a significance threshold of $\alpha = 0.001$, 60/98 genes (61.2%) in the Vogelstein et al. gene set are significantly predictable from gene expression data, compared to 10/107 genes (9.35%) in the random gene set and 43/107 genes (40.2%) in the most mutated gene set. Additionally, Figure 2D shows that many of the significant genes in the most mutated gene set are clustered close to the significance threshold, while the significant genes in the Vogelstein et al. gene set tend to be further from the threshold in Figure 2E (i.e. higher AUPR

differences and lower *p*-values). These results suggest that selecting target genes for mutation prediction based on prior knowledge of their involvement in cancer pathways and processes, rather than randomly or based on mutation frequency alone, can improve predictive signal and identify more highly predictable mutations from gene expression data.
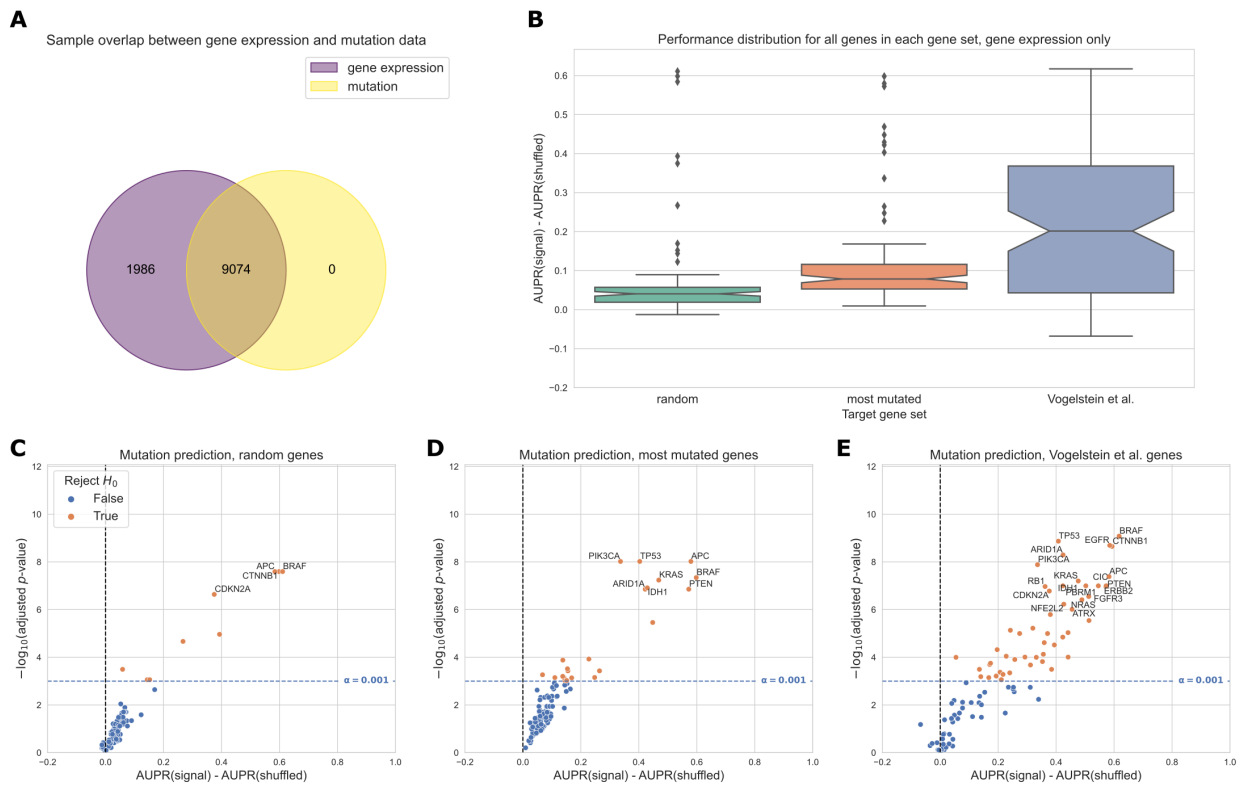

Figure 2: A. Overlap of TCGA samples between gene expression and MC3 somatic mutation data. **B.** Overall distribution of performance across 3 gene sets. Each data point represents mean cross-validated AUPR difference, compared with a baseline model trained on permuted mutation presence/absence labels, for one gene in the given gene set; notches show bootstrapped 95% confidence intervals. "random" = 107 random genes, "most mutated" = 107 most mutated genes, "Vogelstein et al." = 107 cancer related genes from Vogelstein et al. 2013 gene set. **C, D, E.** Volcano-like plots showing mutation presence/absence predictive performance for each gene in each of the 3 gene sets. The *x*-axis shows the difference in mean AUPR compared with a baseline model trained on permuted labels, and the *y*-axis shows *p*-values for a paired *t*-test comparing cross-validated AUPR values within folds.

Comparing six different readouts favors expression and DNA methylation

Next, we expanded our comparison to all five functional data modalities (six total readouts, since there are two DNA methylation datasets) available in the TCGA Pan-Cancer Atlas. As with previous experiments, we limited our comparison to the set of samples profiled for each readout, resulting in 5,226 samples with data for all readouts. The data types with the most missing samples were RPPA data (2,215 samples that were missing RPPA data) and 450K methylation (630 samples that were missing 450K methylation data) (Figure 3A). Summarized over all genes in the Vogelstein et al. dataset, we observed that gene expression and both methylation datasets tended to produce similar quality predictions, and these tended to be slightly better than the remaining data types (Figure 3B). For the set of genes having at least one significant predictor (i.e. "well-predicted" genes), median performance using gene expression was slightly higher than for the methylation data types, although this difference was not statistically significant (Figure 3C).

On the individual gene level, mutations in 25/75 genes were significantly predictable from RPPA data relative to the permuted baseline, compared to 24/75 genes from microRNA data and 3/75 genes from mutational signatures data (Figure 3D-F). For the remaining data types on this smaller set of

samples, 34/75 genes outperformed the baseline for gene expression data, 32/75 for 27k methylation, and 30/75 for 450k methylation. Compared to the methylation experiments shown in Figure ??, we observed slightly fewer "well-predicted" genes for the expression and methylation datasets here (likely due to the considerably smaller sample size) but relative performance was comparable. Direct comparisons between each added data type and gene expression data showed that RPPA data produces comparable or improved predictions for a small number of genes (Figure 3G), but microRNA and mutational signatures data generally provide similar or worse performance (Figure 3H-I). Performance using RPPA data is notable because of its drastically smaller dimensionality than the other data types (190 proteins, compared to thousands of features for the expression and methylation data types), suggesting that each protein abundance measurement provides a high information content. Mutations that are more predictable using RPPA data include *PIK3R1* and *MAP2K1* (Figure 3G). Both genes are kinases involved in phosphorylation-mediated signal transduction. The ability of RPPA technology to quantify protein phosphorylation status may thus provide an advantage in identifying mutations in these genes, relative to the other data types we used that cannot directly measure protein phosphorylation.

When we constructed a heatmap depicting predictive performance for each gene across data types, we found that very few genes tended to be well-predicted exclusively by one or two data types (Figure 4). Of the 39 genes that are well-predicted using at least one data type (blue or red highlighted boxes in Figure 4), only three of them are well-predicted exclusively by a single data type, meaning that mutations in the other 37 genes can be predicted effectively using at least two different data sources. This supports our observation that choosing the "correct" data modality is often unimportant for driver genes with strong functional signatures. Notable exceptions included *NF1* (only well-predicted using gene expression data), *SETD2* (only well-predicted using the two methylation datasets), and *TSC1* (only well-predicted using gene expression data). Gene expression provided the best performance in 25/39 genes with at least one significant data type (red highlighted boxes in Figure 4), but only 2 of those 25 genes did not have any other significantly predictive data types (*NF1* and *TSC1*); in the other 23 genes one or more non-expression data types also outperformed the permuted baseline.
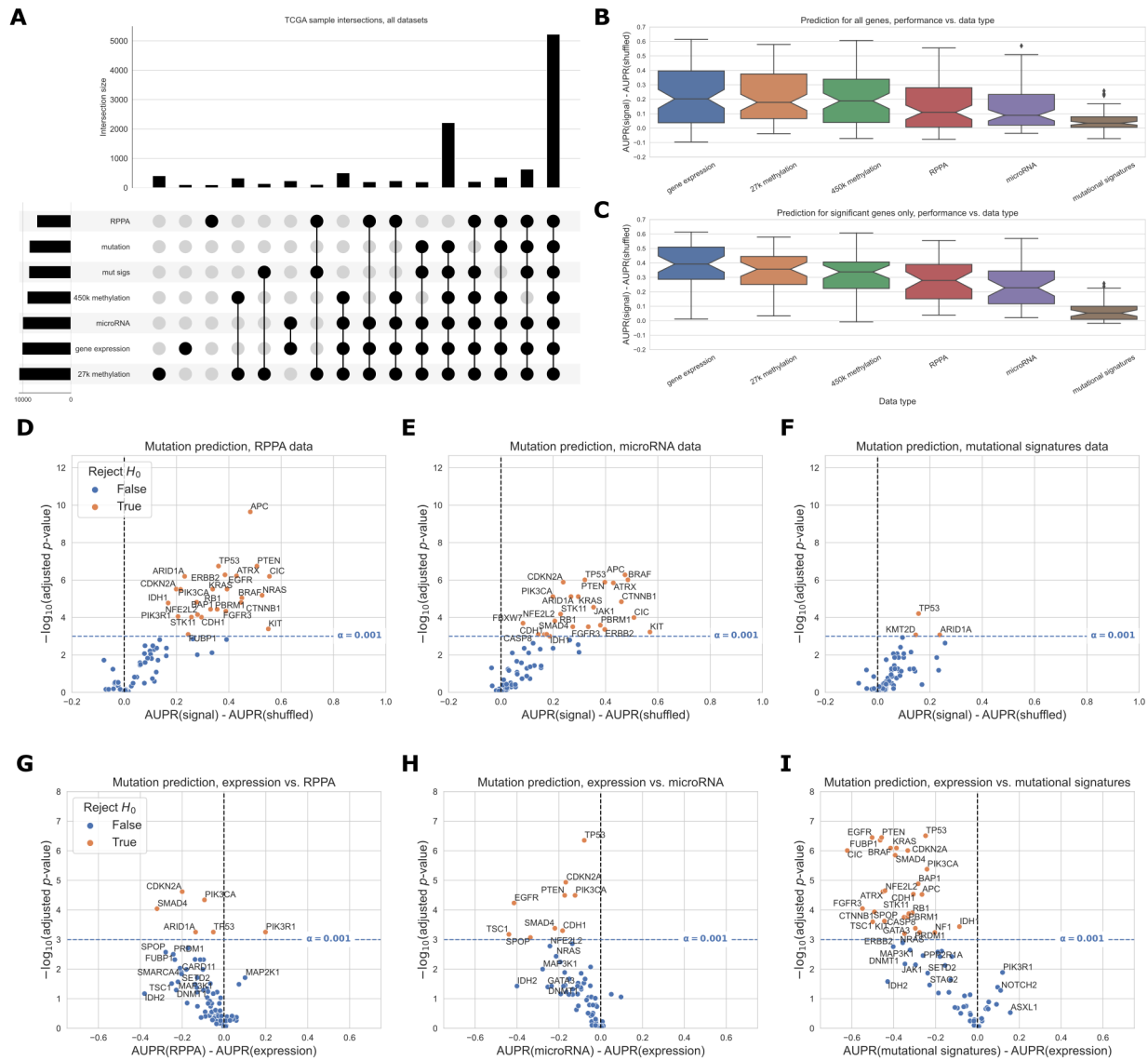
Figure 3: **A.** Overlap of TCGA samples between data types used in mutation prediction comparisons. Only overlaps with more than 100 samples are shown. **B.** Overall distribution of performance per data type across 75 genes from Vogelstein et al. gene set. Each data point represents mean cross-validated AUPR difference, compared with a baseline model trained on permuted labels, for one gene; notches show bootstrapped 95% confidence intervals. **C.** Overall performance distribution per data type for genes where the permuted baseline model is significantly outperformed for one or more data types, resulting in a total of 39 genes. **D, E, F.** Volcano-like plots showing predictive performance for each gene in the Vogelstein et al. gene set, in each of the added data types (RPPA, microRNA, mutational signatures). The x-axis shows the difference in mean AUPR compared with a baseline model trained on permuted labels, and the y-axis shows p-values for a paired t-test comparing cross-validated AUPR values within folds. **G, H, I.** Volcano-like plots comparing predictive performance between data types for each gene in the Vogelstein et al. gene set. The x-axis shows the difference in mean AUPR between gene expression and another data type (positive values = better mean performance using gene expression features), and the y-axis shows p-values for a paired t-test comparing cross-validated AUPR values within folds.
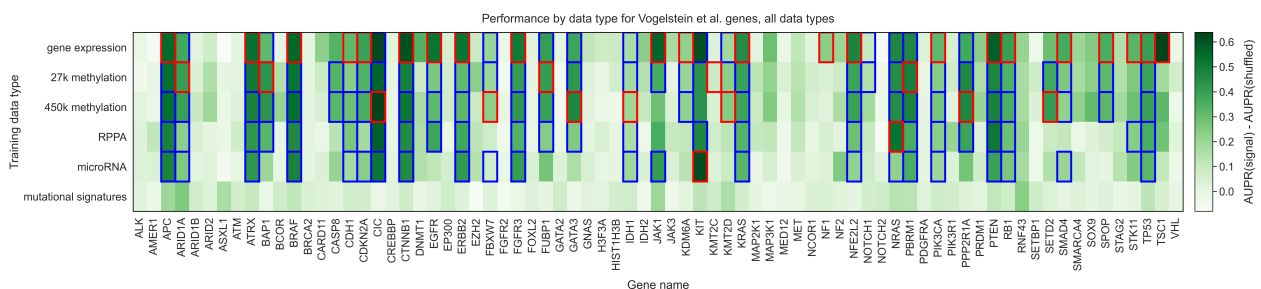
Figure 4: Heatmap displaying predictive performance for mutations in each of the 75 genes from the Vogelstein et al. gene set, across all 6 TCGA data modalities. Each cell quantifies performance for a target gene, using predictive features derived from a particular data type. Blue highlights indicate that the given data type provides significantly

better predictions than the permuted baseline for the given gene; red highlights indicate the same and additionally that the given data type provides the best performance for the given gene, relative to other data types.

References

1. **Oncogenic Signaling Pathways in The Cancer Genome Atlas**
   Francisco Sanchez-Vega, Marco Mina, Joshua Armenia, Walid K. Chatila, Augustin Luna, Konnor C. La, Sofia Dimitriadoy, David L. Liu, Havish S. Kantheti, Sadegh Saghafinia, … Armaz Mariamidze
   Cell (2018-04) https://doi.org/gc7r9b
   DOI: 10.1016/j.cell.2018.03.035 · PMID: 29625050 · PMCID: PMC6070353

2. **Systematic identification of mutations and copy number alterations associated with cancer patient prognosis**
   Joan C Smith, Jason M Sheltzer
   eLife (2018-12-11) https://doi.org/gf4zgg
   DOI: 10.7554/elife.39217 · PMID: 30526857 · PMCID: PMC6289580

3. **Challenges in identifying cancer genes by analysis of exome sequencing data**
   Matan Hofree, Hannah Carter, Jason F. Kreisberg, Sourav Bandyopadhyay, Paul S. Mischel, Stephen Friend, Trey Ideker
   Nature Communications (2016-07-15) https://doi.org/f8x7t3
   DOI: 10.1038/ncomms12096 · PMID: 27417679 · PMCID: PMC4947162

4. **Evaluating the evaluation of cancer driver genes**
   Collin J. Tokheim, Nickolas Papadopoulos, Kenneth W. Kinzler, Bert Vogelstein, Rachel Karchin
   Proceedings of the National Academy of Sciences (2016-12-13) https://doi.org/f9d77w
   DOI: 10.1073/pnas.1616440113 · PMID: 27911828 · PMCID: PMC5167163

5. **Detailed modeling of positive selection improves detection of cancer driver genes**
   Siming Zhao, Jun Liu, Pranav Nanga, Yuwen Liu, A. Ercument Cicek, Nicholas Knoblauch, Chuan He, Matthew Stephens, Xin He
   Nature Communications (2019-07-30) https://doi.org/gjmhnn
   DOI: 10.1038/s41467-019-11284-9 · PMID: 31363082 · PMCID: PMC6667447

6. **Review: Precision medicine and driver mutations: Computational methods, functional assays and conformational principles for interpreting cancer drivers**
   Ruth Nussinov, Hyunbum Jang, Chung-Jung Tsai, Feixiong Cheng
   PLOS Computational Biology (2019-03-28) https://doi.org/gg8jhm
   DOI: 10.1371/journal.pcbi.1006658 · PMID: 30921324 · PMCID: PMC6438456

7. **The Cancer Genome Atlas Pan-Cancer analysis project**
   John N Weinstein, Eric A Collisson, Gordon B Mills, Kenna R Mills Shaw, Brad A Ozenberger, Kyle Ellrott, Ilya Shmulevich, Chris Sander, Joshua M Stuart, The Cancer Genome Atlas Research Network
   Nature Genetics (2013-09-26) https://doi.org/f3nt5c
   DOI: 10.1038/ng.2764 · PMID: 24071849 · PMCID: PMC3919969

8. **Modeling RAS Phenotype in Colorectal Cancer Uncovers Novel Molecular Traits of RAS Dependency and Improves Prediction of Response to Targeted Agents in Patients**
   Justin Guinney, Charles Ferté, Jonathan Dry, Robert McEwen, Gilles Manceau, KJ Kao, Kai-Ming Chang, Claus Bendtsen, Kevin Hudson, Erich Huang, … Pierre Laurent-Puig
   Clinical Cancer Research (2014-01-01) https://doi.org/f5njhn
   DOI: 10.1158/1078-0432.ccr-13-1943 · PMID: 24170544 · PMCID: PMC4141655

9. **Machine Learning Detects Pan-cancer Ras Pathway Activation in The Cancer Genome Atlas**
   Gregory P. Way, Francisco Sanchez-Vega, Konnor La, Joshua Armenia, Walid K. Chatila, Augustin Luna, Chris Sander, Andrew D. Cherniack, Marco Mina, Giovanni Ciriello, … Armaz Mariamidze
   Cell Reports (2018-04) https://doi.org/gfspsb
   DOI: 10.1016/j.celrep.2018.03.046 · PMID: 29617658 · PMCID: PMC5918694

10. **Identification of pan-cancer Ras pathway activation with deep learning**
    Xiangtao Li, Shaochuan Li, Yunhe Wang, Shixiong Zhang, Ka-Chun Wong
    Briefings in Bioinformatics (2020-10-30) https://doi.org/gjmd3p
    DOI: 10.1093/bib/bbaa258 · PMID: 33126245

11. **Genomic and Molecular Landscape of DNA Damage Repair Deficiency across The Cancer Genome Atlas**
    Theo A. Knijnenburg, Linghua Wang, Michael T. Zimmermann, Nyasha Chambwe, Galen F. Gao, Andrew D. Cherniack, Huihui Fan, Hui Shen, Gregory P. Way, Casey S. Greene, … Armaz Mariamidze
    Cell Reports (2018-04) https://doi.org/gfspsc
    DOI: 10.1016/j.celrep.2018.03.076 · PMID: 29617664 · PMCID: PMC5961503

12. **Prediction of PIK3CA mutations from cancer gene expression data**
    Jun Kang, Ahwon Lee, Youn Soo Lee
    PLOS ONE (2020-11-09) https://doi.org/gjmd3s
    DOI: 10.1371/journal.pone.0241514 · PMID: 33166334 · PMCID: PMC7652327

13. **Compressing gene expression data using multiple latent space dimensionalities learns complementary biological representations**
    Gregory P. Way, Michael Zietz, Vincent Rubinetti, Daniel S. Himmelstein, Casey S. Greene
    Genome Biology (2020-05-11) https://doi.org/gg2mjh
    DOI: 10.1186/s13059-020-02021-3 · PMID: 32393369 · PMCID: PMC7212571

14. **Systematic interrogation of mutation groupings reveals divergent downstream expression programs within key cancer genes**
    Michal R. Grzadkowski, Hannah Manning, Julia Somers, Emek Demir
    Cold Spring Harbor Laboratory (2020-06-18) https://doi.org/gjmd7t
    DOI: 10.1101/2020.06.02.128850

15. **Using Transcriptional Signatures to Find Cancer Drivers with LURE**
    David Haan, Ruikang Tao, Verena Friedl, Ioannis N Anastopoulos, Christopher K Wong, Alana S Weinstein, Joshua M Stuart
    World Scientific Pub Co Pte Lt (2019-12) https://doi.org/gjmd4t
    DOI: 10.1142/9789811215636_0031

16. **Reverse regression increases power for detecting trans-eQTLs**
    Saikat Banerjee, Franco L. Simonetti, Kira E. Detrois, Anubhav Kaphle, Raktim Mitra, Rahul Nagial, Johannes Söding
    Cold Spring Harbor Laboratory (2020-09-02) https://doi.org/gjmhd8
    DOI: 10.1101/2020.05.07.083386

17. **Cancer transcriptome profiling at the juncture of clinical translation**
    Marcin Cieślik, Arul M. Chinnaiyan
    Nature Reviews Genetics (2017-12-27) https://doi.org/gcsmnr
    DOI: 10.1038/nrg.2017.96 · PMID: 29279605

18. *IDH1* and *IDH2* Mutations in Gliomas
    Hai Yan, D. Williams Parsons, Genglin Jin, Roger McLendon, B. Ahmed Rasheed, Weishi Yuan, Ivan Kos, Ines Batinic-Haberle, Siân Jones, Gregory J. Riggins, ... Darell D. Bigner
    New England Journal of Medicine (2009-02-19) https://doi.org/btz6db
    DOI: 10.1056/nejmoa0808710 · PMID: 19228619 · PMCID: PMC2820383

19. **IDH mutation impairs histone demethylation and results in a block to cell differentiation**
    Chao Lu, Patrick S. Ward, Gurpreet S. Kapoor, Dan Rohle, Sevin Turcan, Omar Abdel-Wahab, Christopher R. Edwards, Raya Khanin, Maria E. Figueroa, Ari Melnick, ... Craig B. Thompson
    Nature (2012-02-15) https://doi.org/f4msnt
    DOI: 10.1038/nature10860 · PMID: 22343901 · PMCID: PMC3478770

20. **Connections between TET proteins and aberrant DNA modification in cancer**
    Yun Huang, Anjana Rao
    Trends in Genetics (2014-10) https://doi.org/f6jm7v
    DOI: 10.1016/j.tig.2014.07.005 · PMID: 25132561 · PMCID: PMC4337960

21. **SETting the Stage for Cancer Development: SETD2 and the Consequences of Lost Methylation**
    Catherine C. Fahey, Ian J. Davis
    Cold Spring Harbor Perspectives in Medicine (2017-05) https://doi.org/gjmfvq
    DOI: 10.1101/cshperspect.a026468 · PMID: 28159833 · PMCID: PMC5411680

22. **Mechanisms underlying mutational signatures in human cancers**
    Thomas Helleday, Saeed Eshtad, Serena Nik-Zainal
    Nature Reviews Genetics (2014-07-01) https://doi.org/f25gnp
    DOI: 10.1038/nrg3729 · PMID: 24981601 · PMCID: PMC6044419

23. **Quantitative Proteomics of the Cancer Cell Line Encyclopedia**
    David P. Nusinow, John Szpyt, Mahmoud Ghandi, Christopher M. Rose, E. Robert McDonald, Marian Kalocsay, Judit Jané-Valbuena, Ellen Gelfand, Devin K. Schweppe, Mark Jedrychowski, ... Steven P. Gygi
    Cell (2020-01) https://doi.org/ggxbh5
    DOI: 10.1016/j.cell.2019.12.023 · PMID: 31978347 · PMCID: PMC7339254

24. **The repertoire of mutational signatures in human cancer**
    Ludmil B. Alexandrov, Jaegil Kim, Nicholas J. Haradhvala, Mi Ni Huang, Alvin Wei Tian Ng, Yang Wu, Arnoud Boot, Kyle R. Covington, Dmitry A. Gordenin, Erik N. Bergstrom, ... PCAWG Consortium
    Nature (2020-02-05) https://doi.org/ggkfnv
    DOI: 10.1038/s41586-020-1943-3 · PMID: 32025018 · PMCID: PMC7054213

25. **Significant associations between driver gene mutations and DNA methylation alterations across many cancer types**
    Yun-Ching Chen, Valer Gotea, Gennady Margolin, Laura Elnitski
    PLOS Computational Biology (2017-11-10) https://doi.org/gchz8h
    DOI: 10.1371/journal.pcbi.1005840 · PMID: 29125844 · PMCID: PMC5709060

26. **A pan-cancer analysis of driver gene mutations, DNA methylation and gene expressions reveals that chromatin remodeling is a major mechanism inducing global changes in cancer epigenomes**
    Ahrim Youn, Kyung In Kim, Raul Rabadan, Benjamin Tycko, Yufeng Shen, Shuang Wang
    BMC Medical Genomics (2018-11-06) https://doi.org/gjmhfb
    DOI: 10.1186/s12920-018-0425-z · PMID: 30400878 · PMCID: PMC6218985

27. **Computational analysis reveals histotype-dependent molecular profile and actionable mutation effects across cancers**
Daniel Heim, Grégoire Montavon, Peter Hufnagl, Klaus-Robert Müller, Frederick Klauschen
Genome Medicine (2018-11-15) https://doi.org/gjmhfc
DOI: 10.1186/s13073-018-0591-9 · PMID: 30442178 · PMCID: PMC6238410

28. **CNAmet: an R package for integrating copy number, methylation and expression data**
Riku Louhimo, Sampsa Hautaniemi
Bioinformatics (2011-03-15) https://doi.org/fbq4p2
DOI: 10.1093/bioinformatics/btr019 · PMID: 21228048

29. **Impacts of somatic mutations on gene expression: an association perspective**
Peilin Jia, Zhongming Zhao
Briefings in Bioinformatics (2016-04-28) https://doi.org/gjnd5b
DOI: 10.1093/bib/bbw037 · PMID: 27127206 · PMCID: PMC5862283

30. **Inference of patient-specific pathway activities from multi-dimensional cancer genomics data using PARADIGM**
Charles J. Vaske, Stephen C. Benz, J. Zachary Sanborn, Dent Earl, Christopher Szeto, Jingchun Zhu, David Haussler, Joshua M. Stuart
Bioinformatics (2010-06-15) https://doi.org/bcvgjf
DOI: 10.1093/bioinformatics/btq182 · PMID: 20529912 · PMCID: PMC2881367

31. **Systematic analysis of somatic mutations impacting gene expression in 12 tumour types**
Jiarui Ding, Melissa K. McConechy, Hugo M. Horlings, Gavin Ha, Fong Chun Chan, Tyler Funnell, Sarah C. Mullaly, Jüri Reimand, Ali Bashashati, Gary D. Bader, … Sohrab P. Shah
Nature Communications (2015-10-05) https://doi.org/f7z86p
DOI: 10.1038/ncomms9554 · PMID: 26436532 · PMCID: PMC4600750

32. **Cancer Genome Landscapes**
B. Vogelstein, N. Papadopoulos, V. E. Velculescu, S. Zhou, L. A. Diaz, K. W. Kinzler
Science (2013-03-28) https://doi.org/6rg
DOI: 10.1126/science.1235122 · PMID: 23539594 · PMCID: PMC3749880

33. **Scalable Open Science Approach for Mutation Calling of Tumor Exomes Using Multiple Genomic Pipelines**
Kyle Ellrott, Matthew H. Bailey, Gordon Saksena, Kyle R. Covington, Cyriac Kandoth, Chip Stewart, Julian Hess, Singer Ma, Kami E. Chiotti, Michael McLellan, … Armaz Mariamidze
Cell Systems (2018-03) https://doi.org/gf9twn
DOI: 10.1016/j.cels.2018.03.002 · PMID: 29596782 · PMCID: PMC6075717

34. **GISTIC2.0 facilitates sensitive and confident localization of the targets of focal somatic copy-number alteration in human cancers**
Craig H Mermel, Steven E Schumacher, Barbara Hill, Matthew L Meyerson, Rameen Beroukhim, Gad Getz
Genome Biology (2011-04-28) https://doi.org/dzhjqh
DOI: 10.1186/gb-2011-12-4-r41 · PMID: 21527027 · PMCID: PMC3218867

35. **Scikit-learn: Machine Learning in Python**
Fabian Pedregosa, Gaël Varoquaux, Alexandre Gramfort, Vincent Michel, Bertrand Thirion, Olivier Grisel, Mathieu Blondel, Peter Prettenhofer, Ron Weiss, Vincent Dubourg, … Édouard Duchesnay
Journal of Machine Learning Research (2011) http://jmlr.org/papers/v12/pedregosa11a.html

36. **A beta-mixture quantile normalization method for correcting probe design bias in Illumina Infinium 450 k DNA methylation data**
Andrew E. Teschendorff, Francesco Marabita, Matthias Lechner, Thomas Bartlett, Jesper Tegner, David Gomez-Cabrero, Stephan Beck
Bioinformatics (2013-01-15) https://doi.org/f25mvt
DOI: 10.1093/bioinformatics/bts680 · PMID: 23175756 · PMCID: PMC3546795

37. **Regularization and variable selection via the elastic net**
Hui Zou, Trevor Hastie
Journal of the Royal Statistical Society: Series B (Statistical Methodology) (2005-04)
https://doi.org/b8cwwr
DOI: 10.1111/j.1467-9868.2005.00503.x

38. **An introduction to ROC analysis**
Tom Fawcett
Pattern Recognition Letters (2006-06) https://doi.org/bpsghb
DOI: 10.1016/j.patrec.2005.10.010

39. **A critical investigation of recall and precision as measures of retrieval system performance**
Vijay Raghavan, Peter Bollmann, Gwang S. Jung
ACM Transactions on Information Systems (1989-07) https://doi.org/bg4tps
DOI: 10.1145/65943.65945

40. **The Precision-Recall Plot Is More Informative than the ROC Plot When Evaluating Binary Classifiers on Imbalanced Datasets**
Takaya Saito, Marc Rehmsmeier
PLOS ONE (2015-03-04) https://doi.org/f69237
DOI: 10.1371/journal.pone.0118432 · PMID: 25738806 · PMCID: PMC4349800

41. **The MCC-F1 curve: a performance evaluation technique for binary classification**
Chang Cao, Davide Chicco, Michael M. Hoffman
arXiv (2020-06-23) https://arxiv.org/abs/2006.11278